RJC

RASĀYAN *J. Chem.*
Vol. 17 | No. 1 |38-46| January - March | 2024
ISSN: 0974-1496 | e-ISSN: 0976-0083 | CODEN: RJCABP
http://www.rasayanjournal.com
http://www.rasayanjournal.co.in

STRUCTURE, QUANTUM CHEMICAL, HIRSHFELD SURFACES, AND ENERGY FRAMEWORK ANALYSIS OF SOME AMINOPYRIDINE DERIVATIVES

R. Sharma[1] and R. Kant[1,2,✉]

[1]Department of Physics, University of Jammu, Jammu Tawi-180006, (Jammu & Kashmir) India
[2]Vice-Chancellor, Rabindranath Tagore University, Bhopal-464993, (Madhya Pradesh) India
✉Corresponding Author: rkant.ju@gmail.com

ABSTRACT

The X-ray crystal structures of some aminopyridine derivatives as contained in CSD have been examined for structure optimization and quantum chemical analysis. The experimental data and quantum chemical analysis uncover intriguing findings. The research extensively explores optimized structural geometry, the frontier orbital energy gap, the distribution of atomic Mulliken charges, and the molecular electrostatic potential (MEP). The Hirshfeld surfaces and their 2D fingerprint plots confirm the existence of N-H... N, O-H…N, and N-H…O intermolecular interactions in the molecules. The void volume percentage, which has been calculated to determine the physical strength of each molecule, is generally consistent among all the identified molecules. The energy frameworks reveal that electrostatic energy emerges as the dominant factor in each structure.

Keywords: Aminopyridines, Density Functional Theory, Hirshfeld Surface, Crystal Voids, Energy Frameworks.
RASĀYAN *J. Chem.*, Vol. 17, No.1, 2024

INTRODUCTION

Aminopyridines have garnered significant attention in recent decades due to their intriguing biological properties found in synthetic and natural compounds.[1,2] Among the numerous 6-membered heterocyclic compounds, aminopyridines stand out for their diverse pharmacological activities linked to their presence in targeted molecules.[3] Research has demonstrated that the inclusion of a small aminopyridine moiety confers medicinal advantages to the target molecule, whether it is a simple compound with few functional groups or a complex one containing multiple heterocyclic structures.[4,5] Aminopyridine is an organic compound characterized by the presence of an amino group and an aromatic heterocyclic pyridine ring. It finds applications as reagents and catalysts in organic synthesis and the fields of dyes and nonlinear optical materials.[6] In the pharmaceutical industry, various derivatives of aminopyridine serve as crucial precursors for the production of antibacterial, and antiviral drugs, herbicides, and dyes.[7,8] Aminopyridines with antibacterial and antithrombotic properties have proven important in the treatment of various medical conditions.[9] One such example is 4-aminopyridine, which stands as the pioneering pharmacological molecule known for its efficacy in treating multiple sclerosis syndromes through the modulation of potassium channels.[10] Given some diverse properties exhibited by aminopyridine derivatives, we have chosen a series of chemically analogous aminopyridine derivatives to facilitate a comprehensive comparative analysis of X-ray structures and allied structural properties using the Gaussian 09 program.[11] The crystal structures as identified from the CSD (version 2022) search are coded as AMEPYD (2-amino-4-methylpyridine), AMNTPY (2-amino-3-nitropyridine), EXIQOS (2-Aminopyridin-3-ol) and FOYLEK01(2,6-Diaminopyridine).[12-15] The Hirshfeld surface analysis and energy frameworks have been examined using the Crystal Explorer 21.5 program to assess the stability of the molecules concerning crystal packing.[16] The chemical structures of the identified molecules are shown in Fig.-1. The precise crystallographic data are presented in Table-1.

EXPERIMENTAL

DFT Calculations

Density Functional Theory (DFT) method has been used for structure optimization, employing the 6-311++G(d, p) basis set. A comparison has been made between the optimized geometrical parameters (bond distances and bond angles) with their corresponding experimental values. These optimized

http://doi.org/10.31788/RJC.2024.1718667

parameters have been used for the computation of Mulliken charges, the HOMO-LUMO energy gap, molecular electrostatic potential maps, and various other molecular properties. All computational procedures have been executed using the Gaussian 09W software.[11]

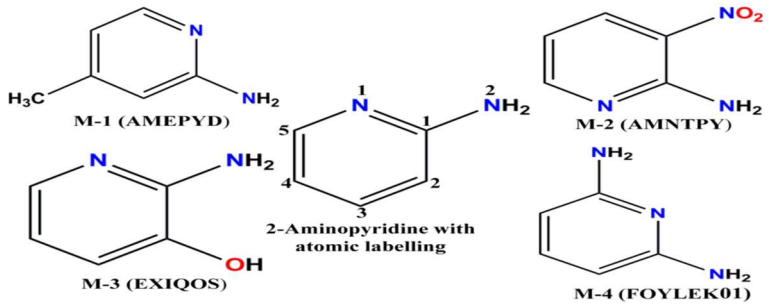

Fig.-1: Chemical Structures of the Identified Aminopyridine Derivatives

Table-1: Precise Crystallographic Data of Each Structure

Parameters	M-1[12]	M-2[13]	M-3[14]	M-4[15]
CCDC code	AMEPYD	AMNTPY	EXIQOS	FOYLEK01
Chemical Formula	$C_6H_8N_2$	$C_5H_5N_3O_2$	$C_5H_6N_2O$	$C_5H_7N_3$
Radiation used	Cu K_α	Cu K_α	Mo K_α	Mo K_α
Temperature (K)	100	153	200	100
Crystal system	Orthorhombic	Monoclinic	Monoclinic	Orthorhombic
Space group	*Pbca*	$P2_1/c$	$P2_1/c$	*Pbca*
Lattice parameters (Å, °)	a = 27.06(1) b = 7.309(1) c = 5.849(3) α = 90.00 β = 90.00 γ = 90.00	a = 4.917(1) b = 6.940(2) c = 17.507(3) α = 90.00 β = 95.63(2) γ = 90.00	a = 12.531(6) b = 3.889(2) c = 11.604(5) α = 90.00 β = 113.14(2) γ = 90.00	a = 5.1217 (9) b = 9.8397 (1) c = 21.914 (4) α = 90.00 β = 90.00 γ = 90.00
Unit cell volume(Å^3)	1156.9	594.5(2)	519.9(4)	1104.4(3)
Z	8	4	4	8
R-factor	4.10	5.75	3.64	5.60

Hirshfeld Surface Calculations

The Hirshfeld surface (HS) is a region surrounding a molecule within a crystalline structure, serving as a boundary that separates the inner reference molecule from its neighboring outer molecule. This separation within crystal space allows for the examination of intermolecular interactions through distinctive features, or "fingerprints".[17,18] HS analysis is a valuable tool for visualizing and quantifying various non-covalent interactions responsible for stabilizing the arrangement of molecules in a crystal. The HS can be described using d_{norm}, shape index, and curvature. On the d_{norm} surface, red and blue regions denote shorter and longer intermolecular contacts, respectively, whereas white areas correspond to contacts occurring at the van der Waals radii. The fingerprint plots are employed to convey pertinent information regarding intermolecular contacts in the crystal structure.

To conduct HS analyses and generate associated 2D fingerprint plots, the Crystal Explorer 21.5 program is utilized.[16,19] These analyses require a crystallographic information file (CIF) as input. Additionally, for consistency, the bond lengths involving hydrogen atoms participating in interactions are normalized to standard neutron values (C-H = 1.083 Å, N-H = 1.009 Å, O-H = 0.983 Å). The HS method employs the isosurface corresponding to a molecular electron density of 0.002 atomic units to visually represent voids or spaces within the crystal structure.[20-23]

Energy Framework Study

The energy framework quantification method provides valuable insights into the molecular interactions within a crystal, allowing for a comprehensive understanding of its topology.[24] This method involves the calculation and comparison of various energy components, including repulsion (E_{rep}), electric (E_{ele}), dispersion (E_{dis}), polarization (E_{pol}), and total energy (E_{tot}). These calculations are based on the anisotropy

of the pairwise intermolecular interaction energies. In this study, the Crystal Explorer program version 21.5 was employed to determine the energy framework of aminopyridine derivatives.[16] This was accomplished by generating new wave functions using the Density Functional Theory (DFT) method with a 3-21G basis set, incorporating exchange and potential functions (B3LYP), and simulating a molecular cluster environment within a 1x1x1 unit cell. The thickness of the cylindrical radius within the visualization represents the strength of interactions and is directly correlated with the magnitude of energy associated with those interactions. This information offers valuable insights into the stability of the crystal packing arrangement.

RESULTS AND DISCUSSION

Molecular Geometry

The molecular geometry optimization has been performed on all four structures using the DFT method with the B3LYP/6-311++G(d,p) basis set and their optimized structures are shown in Fig.-2. A comparative analysis was conducted between the bond distances and angles obtained from theoretical calculations and those determined experimentally through X-ray structure analysis. The findings, as outlined in Table-2, reveal a favorable correspondence between the experimental and theoretical values.

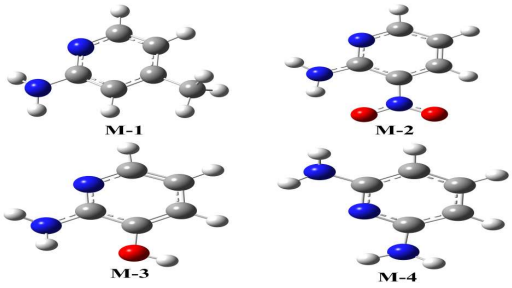

Fig.-2: Geometrically Optimized Structures (M-1 to M-4)

Table-2: Bond Distances (Å) and Angles (°): X-ray vs. DFT

Atoms	M-1 (AMEPYD)		M-2 (AMNTPY)		M-3 (EXIQOS)		M-4 (FOYLEK01)	
	XRD	DFT	XRD	DFT	XRD	DFT	XRD	DFT
N1 – C1	1.347	1.336	1.359	1.352	1.331	1.330	1.347	1.338
N1 – C5	1.348	1.338	1.325	1.323	1.349	1.341	1.349	1.338
N2 – C2	1.363	1.384	1.331	1.347	1.367	1.377	1.378	1.384
C1 – C2	1.410	1.409	1.421	1.426	1.422	1.416	1.403	1.405
C2 – C3	1.383	1.387	1.394	1.395	1.371	1.379	1.397	1.389
C3 – C4	1.397	1.405	1.363	1.381	1.399	1.401	1.392	1.389
C4 – C5	1.382	1.386	1.406	1.400	1.368	1.386	1.395	1.405
N1 – C1 – N2	116.4	116.3	115.3	115.6	118.7	118.5	116.1	115.8
C2 – C1 – N2	121.5	121.0	125.6	124.6	119.5	119.7	121.2	121.3
C1 – N1 – C5	117.3	117.4	119.4	119.4	118.7	118.8	118.6	118.7
N1 – C1 – C2	122.0	122.6	119.1	119.8	121.7	121.7	122.7	122.9
N1 – C5 – C4	124.1	124.2	124.1	124.3	123.1	123.4	122.9	122.8
C1 – C2 – C3	119.7	119.5	120.1	119.5	118.3	118.9	117.9	117.5
C2 – C3 – C4	118.2	117.7	119.7	119.5	119.5	119.0	120.6	120.5
C3 – C4 – C5	118.6	118.6	117.5	117.4	118.5	118.0	117.7	117.5

Frontier Molecular Orbitals (FMO) Analysis

The electric and optical parameters of the structure in the Frontier Molecular Orbitals (FMO) theory were computed by using the B3LYP/6-311++G(d,p) basis set. The highest and lowest orbitals are conventionally the FMOs and they exhibit charge density i.e., localized around the aminopyridine ring in the case of all the structures.[25,26] This localization pattern provides valuable insights into molecular characteristics.[27,28] The molecule M-1 demonstrates a significant HOMO-LUMO energy gap with a value of ΔE = 5.37 eV. This substantial gap indicates a high level of stability, suggesting that the molecule is a hard system resistant to chemical reactions. Similarly, the molecules M-3 and M-4 are hard molecules

with high stability and less reactivity. Conversely, in the case of molecule M-2, the HOMO-LUMO energy gap is relatively small (ΔE = 3.94 eV), indicating its inherent instability and heightened reactivity, providing insight into the occurring charge transfer interactions within the molecule (Fig.-3). The various global reactivity parameters are listed in Table-3.

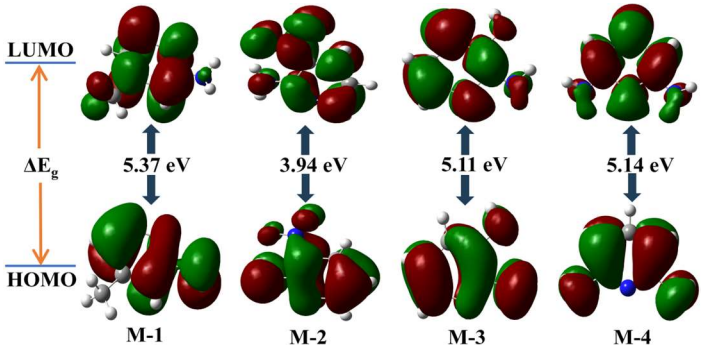

Fig.-3: HOMO-LUMO Energy Gaps

Table-3: Various Global Reactivity Parameters of M-1 to M-4

Reactivity parameters	M-1	M-2	M-3	M-4
E_{HOMO} (eV)	-6.04	-6.90	-5.82	-5.54
E_{LUMO} (eV)	-0.67	-2.96	-0.71	-0.40
$\Delta E = (E_{LUMO} - E_{HOMO})$ (eV)	5.37	3.94	5.11	5.14
Hardness, $\eta = \Delta E/2$ (eV)	2.68	1.97	2.55	2.57
Softness, $\sigma = 1/2\eta$ (eV^{-1})	0.19	0.25	0.19	0.19
Chemical Potential, ($\mu = (E_{LUMO} + E_{HOMO})/2$) (eV)	-3.35	-4.93	-3.26	-2.97
Electrophilicity Index, $\omega = \mu^2/2\eta$ (eV)	2.09	6.17	2.08	1.72
Electronegativity, $\chi = -\mu$ (eV)	3.35	4.93	3.26	2.97

MEP Maps and Mulliken Atomic Charges

The Molecular Electrostatic Potential and atomic charges were computed using DFT/B3LYP/6-311+G(d,p). In Fig.-4, the negative regions (colored red) are predominantly situated around the nitrogen atoms in molecules M-1 and M-4 whereas in the case of molecule M-3, the negative region is primarily centered on the nitro group. In molecules M-1, M-2, and M-3, the positive areas (colored blue) are centered about the hydrogen atoms of the amine group, while in the case of M-2, this positive region extends to cover both the amine and hydroxyl groups. The Mulliken plot, as shown in Fig.-5, illustrates that all nitrogen atoms in the molecules (M1–M4) carry a negative charge. The carbon atoms in all the molecules, generally, exhibit negative charges, except for atom C2 (in M-1, M-3, and M-4), C3 (in M-1 and M-2), and C4 (in M-4). The MEP and Mulliken charge analyses provide valuable insights into the electrophilic and nucleophilic sites within these molecules shedding light on their reactivity and potential for chemical interactions.

Hirshfeld Surface Analysis and Fingerprint Plots

HS analysis has emerged as a valuable tool for elucidating the nature of intermolecular interactions that impact the arrangement of molecules within crystals.[29] In Fig.-6, the d_{norm} plots illustrate distinct red regions that represent various intercontacts present in each crystal structure. The size of these red spots provides insight into the strength of these interactions.[17,18] The observed red spots on the d_{norm} plot indicate N-H...N contacts in the molecules M-1 and M-4 whereas M-2 shows N-H...N, and N-H...O interactions. The significant red spots on the d_{norm} surface of molecule M-3 signify strong intermolecular N-H...N, O-H…N, and N-H…O hydrogen bonds. The HS has been plotted on a shape index and curvedness map to visualize the non-covalent (stacking) interactions. The existence of convex blue regions (donor groups) and concave red regions (acceptor groups) on the shape index indicates the presence of C−H···π interactions in the crystal structures whereas the curved surface indicates the non-existence of π−π planar stacking contacts (Fig.-6).

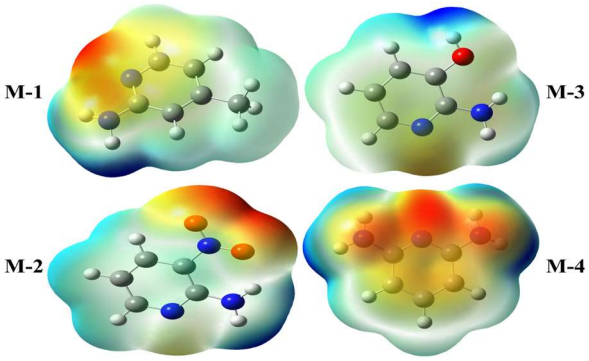

Fig.-4: Molecular Electrostatic Map of Each Molecule

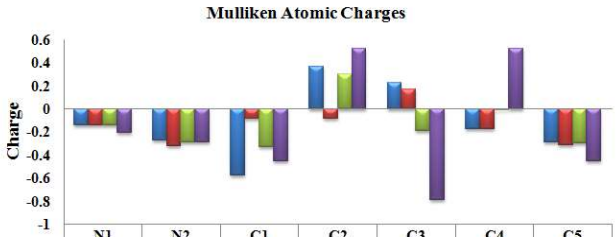

	N1	N2	C1	C2	C3	C4	C5
M-1	-0.139	-0.275	-0.578	0.367	0.226	-0.174	-0.292
M-2	-0.144	-0.324	-0.085	-0.088	0.171	-0.174	-0.317
M-3	-0.147	-0.293	-0.334	0.299	-0.19	-0.011	-0.301
M-4	-0.205	-0.294	-0.455	0.521	-0.794	0.52	-0.454

Fig.-5: Comparison of Mulliken Charge Analysis of Each Molecule

The void analysis has been carried out by utilizing a pro crystal electron density isosurface (0.002 au) employed in the Crystal Explorer 21.5 program.[16] The crystal voids of all the molecules are depicted in Fig.-7. The void volume percentage for M-1 (7.6%) and M-2 (7.5%) is nearly identical, while for M-3 and M-4, it is 8.5% and 2.0%, respectively. This variation in void percentages suggests that M-4 possesses better physical strength, followed by M-2, M-1, and M-3.

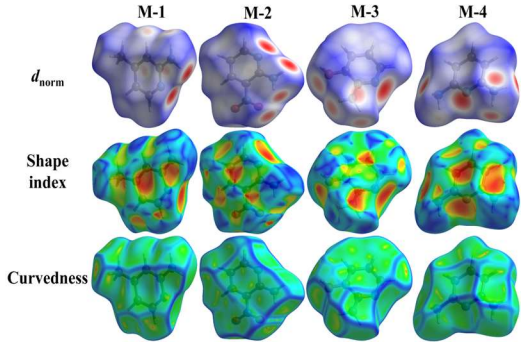

Fig.-6: Comparison of d_{norm} Surfaces, Shape Index, and Curvedness Plots of Each Molecule

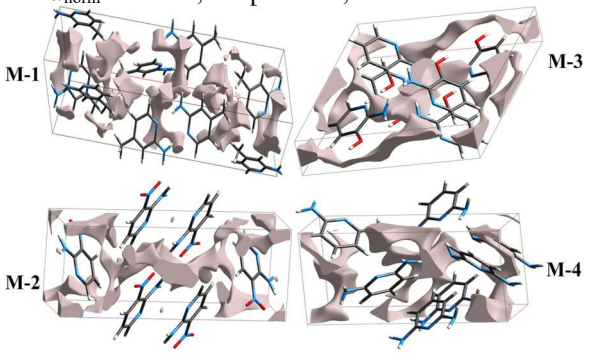

Fig.-7: Crystal Voids of Each Molecule at (0.002 au)-Isosurface

The unique characteristics of intermolecular contacts, as observed on the Hirshfeld surface, are effectively visualized through 2D fingerprint plots. These plots provide valuable insights into the contribution of different interactions to the total Hirshfeld surface area, as demonstrated in Fig.-8. The hydrogen-bonded interactions are depicted as distinct spikes, with the sharpness of each peak and its corresponding $d_i + d_e$ value indicating the relative strength of these interactions. In all the molecules under investigation, the fingerprint plots consistently reveal sharp spikes, which correspond to N…H/H…N contacts. The H...H interactions are observed at the center of dispersed spots within the plots (Fig.-8). The presence of distinct "butterflies" within the fingerprint plots is attributed to C...H contacts, providing a comprehensive visualization of the various intermolecular interactions within the crystal structures.

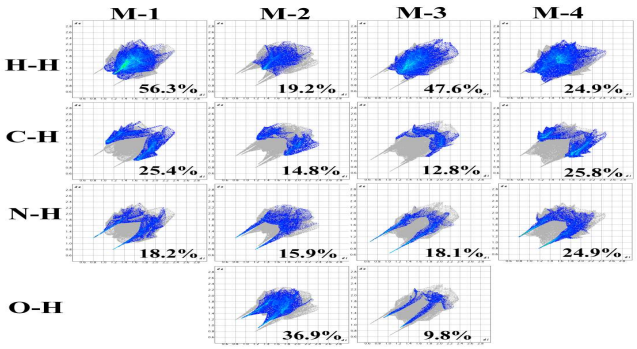

Fig.-8: 2D-Fingerprint Plots Showing Close Contacts of Each Molecule (M-1 to M-4)

Energy Framework Analysis

The intermolecular interaction energies are calculated using the HF/3-21G energy model with scale factors to determine E_{tot}: $k_{ele} = 1.019$, $k_{pol} = 0.651$, $k_{dis} = 0.901$, $k_{rep} = 0.811$.[30] Energy interactions between pairs of molecules are visualized through cylinders connecting the centroids of the molecule pairs. The radius of each cylinder is proportional to the relative strength of the corresponding interaction energy.[31-34] The interactions between various pairs of molecules were dissected into distinct components, including electrostatics (E_{ele}), polarization (E_{pol}), dispersion (E_{dis}), and repulsion (E_{rep}). These components are presented in Table-4 for all the structural configurations. The net interaction energies (E_{tot}) for M-1 and M-3 are nearly indistinguishable, both at approximately -122.2 kJ/mol and -122.7 kJ/mol, respectively. However, for M-2 and M-4, the total interaction energies differ significantly, standing at -142.7 kJ/mol and -104.1 kJ/mol, respectively. This discrepancy primarily arises from variations in their electrostatic energy. The electrostatic energy emerges as the dominant factor in all structures. A visual representation of this dominance is shown in Fig.-9, specifically along the a-axis. In molecule M-3, the interactions for coulomb energy and dispersion energy are strong between the molecules, whereas the interactions for dispersion energy in M-2 and total energy in M-3 are weak. Similarly, the interactions for the coulomb energy in M-2 and the total energy in M-4 are strongest from the centroid of the molecular pairs towards the left side.

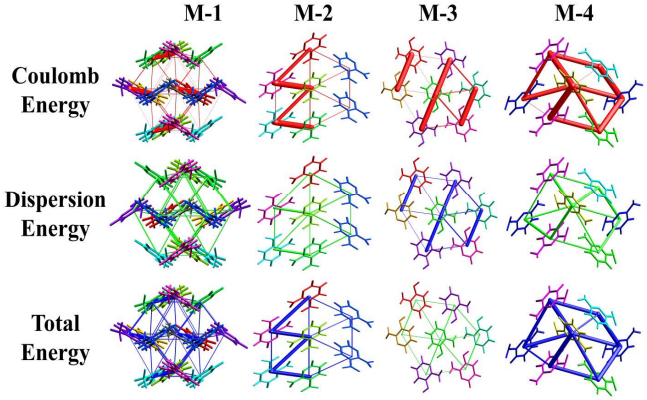

Fig.-9: Graphical View of Coulomb (red), Dispersion (green), and Total Interaction Energy (Blue) Along the x-Axis

Table-4: Interaction Energies in kJ/mol using B3LYP/6-31 G(d, p) Method

Color	N	Symop		R	E_ele	E_pol	E_dis	E_rep	E_tot
M1									
	1	-x, -y, -z		6.36	-73.4	-17.7	-15.8	83.6	-52.9
	1	-x, -y, -z		6.98	-4.3	-0.9	-7.5	4.0	-9.2
	2	-x, y+1/2, -z+1/2		7.02	-6.6	-0.9	-5.5	1.3	-11.6
	2	x, -y+1/2, z+1/2		4.40	-9.1	-3.1	-29.4	25.9	-21.5
	2	x, -y+1/2, z+1/2		4.98	-1.8	-0.9	-17.9	13.9	-9.5
	2	-x+1/2, -y, z+1/2		8.14	-0.6	-0.1	-6.8	3.9	-4.3
	2	x, y, z		5.85	-4.9	-0.7	-11.1	6.7	-11.3
	2	-x+1/2, y+1/2, z		8.42	0.1	-0.1	-3.3	1.6	-1.9
M2									
	2	x, y, z		8.51	-4.5	-1.2	-3.6	2.6	-7.2
	2	-x, y+1/2, -z+1/2		7.07	-6.1	-2.1	-7.6	9.1	-9.0
	2	x, y, z		4.92	-0.3	-1.1	-20.8	11.7	-12.0
	2	x, y, z		6.94	-2.4	-1.1	-8.0	3.9	-7.9
	1	-x, -y, -z		6.65	-32.1	-5.1	-9.5	21.4	-32.8
	2	-x, y+1/2, -z+1/2		5.90	0.5	-0.8	-12.8	6.5	-7.2
	1	-x, -y, -z		4.34	-3.7	-1.1	-30.0	16.2	-20.9
	1	-x, -y, -z		6.60	-68.4	-15.1	-16.8	84.8	-45.7
M3									
	1	-x, -y, -z		7.57	-2.3	-0.2	-8.2	6.3	-5.8
	2	-x, y+1/2, -z+1/2		6.79	-2.5	-0.4	-7.7	5.3	-6.4
	2	x, -y+1/2, z+1/2		7.27	-0.5	-0.3	-1.8	0.0	-2.3
	2	x, y, z		3.89	-0.2	-1.9	-26.4	13.6	-16.2
	2	-x, y+1/2, -z+1/2		6.44	-13.0	-2.9	-9.0	17.7	-12.8
	2	x, -y+1/2, z+1/2		5.82	-83.6	-20.8	-15.8	107.4	-51.1
	1	-x, -y, -z		6.39	-19.9	-2.5	-11.9	26.2	-17.1
	2	x, -y+1/2, z+1/2		6.72	-1.8	-0.7	-5.0	2.5	-5.2
	1	-x, -y, -z		6.09	-1.5	-0.5	-4.6	0.2	-5.8
M4									
	2	-x, y+1/2, -z+1/2		5.64	-37.3	-7.9	-18.5	51.3	-29.8
	2	x, y, z		5.40	-1.3	-1.2	-15.1	9.6	-9.4
	2	x+1/2, -y+1/2, -z		6.83	-20.6	-3.1	-10.0	18.2	-21.6
	2	x+1/2, -y+1/2, -z		5.21	-1.6	-0.9	-17.3	11.8	-10.2
	2	-x+1/2, -y, z+1/2		6.94	-26.3	-5.5	-10.2	32.0	-21.0
	2	-x, y+1/2, -z+1/2		5.29	-3.0	-1.3	-15.1	8.3	-12.1

CONCLUSION

This work focuses on the theoretical exploration of crystal structures in aminopyridine derivatives, accompanied by a thorough examination of their Hirshfeld surfaces and energy framework analyses. Overall, the DFT-optimized geometries closely align with X-ray parameters, ensuring consistency. The DFT investigations yield valuable insights into the molecular structure including Mulliken charges, MEP, and HOMO-LUMO gaps for each molecule. The frontier molecular orbital analysis highlights that M-2 exhibits a greater propensity for charge transfer compared to the other molecules. The Hirshfeld surface analysis uncovers the presence of N-H...N, N-H...O, and O-H...N interactions within the molecules. An essential finding from the 3D energy framework analysis is that electrostatic energy predominates over the dispersion component, demonstrating a substantial contribution of the electrostatic component in each molecule.

ACKNOWLEDGMENTS

Rajni Kant acknowledges the financial support received from the University of Jammu for the licensed access of CSD.

CONFLICT OF INTERESTS

The authors declare that there is no conflict of interest.

AUTHOR CONTRIBUTIONS

All the authors contributed significantly to this manuscript, participated in reviewing/editing, and approved the final draft for publication. The research profile of the authors can be verified from their ORCID IDs, given below:

R. Sharma https://orcid.org/0000-0002-5698-4067
R. Kant https://orcid.org/0000-0001-8043-2329

REFERENCES

1. S. K. Nechipadappu and D. R. Trivedi, *Journal of Molecular Structure,* **1141,** 64(2017), https://doi.org/10.1016/j.molstruc.2017.03.086
2. A. A. Altaf, A. Shahzad, Z. Gul, N. Rasool, A. Badshah, B. Lal and E. Khan, *Journal of Drug Design and Medicinal Chemistry,* **1,** 1(2015), https://doi.org/10.11648/j.jddmc.2 0150101.11
3. K. J. Orie, R. U. Duru and R. I-oro Ngochindo, *American Journal of Heterocyclic Chemistry*, **7(2)**, 11(2021), https://doi.org/10.11648/j.ajhc.20210702.11
4. C. Donlawson, D. O. Nweneka, K. J. Orie and R. Okah, *American Journal of Analytical Chemistry,* **11(7),** 280(2020), https://doi.org/10.4236/ajac.2020.117022
5. M. Vamos and N. D. Cosford, *The Journal of Organic Chemistry,* **79(5),** 2274(2014), https://doi.org/10.1021/jo402693s
6. M. N. Esaulkov, M. I. Fokina, N. A. Zulina, T. V. Timofeeva, A. P. Shkurinov and I. Y. Denisyuk, *Optics & Laser Technology,* **108,** 450(2018), https://doi.org/10.1016/j.optlastec.2018.07.033
7. S. Lakrout, H. K'tir, A. Amira, M. Berredjem, and N. E. Aouf, *RSC Advances,* **4(31),** 16027(2014), https://doi.org/10.1039/C4RA01346H
8. M. Asif, *International Journal of Bioorganic Chemistry,* **2(3),** 146(2017), https://doi.org/10.11648/j.ijbc
9. K. M. Al-Ahmary, M. M. Habeeb and E. A. Al-Solmy, *Journal of Molecular Liquids*,**162**, 129(2011), https://doi.org/10.1016/j.molliq.2011.06.015
10. A. G. E. Amr, A. M. Mohamed, S. F. Mohamed, N. A. Abdel-Hafez and A. E. F. G. Hammam, *Bioorganic and Medicinal Chemistry,* **14,** 5481(2006), https://doi.org/10.1016/j.bmc.2006.04.045
11. A. Frisch, *Gaussian 09W Reference*, (Wallingford, USA, 2009) p. 25.
12. A. Kvick and J. Noordik, *Acta Crystallographica Section B: Structural Science, Crystal Engineering and Materials,* **33,** 2862(1977), https://doi.org/10.1107/S056774087700964 9
13. R. Destro, T. Pilati and M. Simonetta, *Acta Crystallographica Section B: Structural Science, Crystal Engineering and Materials,* **31,** 2883(1975), https://doi.org10.1107/ S0567740875009120
14. R. Betz, T. Gerber, E. Hosten and H. Schalekamp, *Acta Crystallographica Section E: Structure Reports Online*, **67,** o2513(2011), https://doi.org/10.1107/S1600536811034775
15. V. M. Hall, J. A. Bertke and J. A. Swift, *Acta Crystallographica Section C: Structural Chemistry*, **73,** 990(2017), https://doi.org/10.1107/S2053229617014978
16. P. R. Spackman, M. J. Turner, J. J. McKinnon, S. K. Wolff, D. J. Grimwood, D. Jayatilaka and M. A. Spackman, *Journal of Applied Crystallography,* **54,** 1006(2021), https://doi.org/10.1107/S1600576721002910
17. J. J. McKinnon, D. Jayatilaka and M. A. Spackman, *Chemical Communications,* **37,** 3814(2007), https://doi.org/10.1039/B704980C
18. M. A. Spackman and D. Jayatilaka, *CrystEngComm,* **11,** 19(2009), https://doi.org/10.1039/B818330A
19. M. A. Spackman and J. J. McKinnon, *CrystEngComm,* **4,** 378(2012), https://doi.org/10.1039/B203191B
20. M. J. Turner, J. J. McKinnon, D. Jayatilaka and M. A. Spackman, *CrystEngComm,* **13(6),**

1804(2011), https://doi.org/10.1039/C0CE00683A
21. H. Kargar, M. Fallah-Mehrjardi, R. Behjatmanesh-Ardakani, K. S. Munawar, M. Ashfaq and M. N. Tahir, *Journal of Molecular Structure,* **1241,** 130653(2021), https://doi.org/10.1016/j.molstruc.2021.130653
22. H. Kargar, M. Fallah-Mehrjardi, R. Behjatmanesh-Ardakani, M. N. Tahir, M. Ashfaq and K. S. Munawar, *Journal of Coordination Chemistry,* **74,** 2682(2021), https://doi.org/10.1080/00958972.2021.1972984
23. H. Kargar, M. Fallah-Mehrjardi, R. Behjatmanesh-Ardakani, K. S. Munawar, M. Ashfaq and M. N. Tahir, *Journal of Molecular Structure,* **1250,** 131691(2022), https://doi.org/10.1016/j.molstruc.2021.131691
24. M. J. Turner, S. P. Thomas, M. W. Shi, D. Jayatilaka, M. A. Spackman, *Chemical Communication,* **51**, 3735, (2015), https://doi.org/10.1039/C4CC09074H
25. C. Alaşalvar, *Spectrochimica Acta, Part A: Molecular and Biomolecular Spectroscopy,* **132,** 555(2014), https://doi.org/10.1016/j.saa.2014.05.014
26. A. C. Ekennia, A. A. Osowole, L. O. Olasunkanmi, D. C. Onwudiwe, O. O. Olubiyi and E. E. Ebenso, *Journal of Molecular Structure,* **1150,** 279(2017), https://doi.org/10.1016/j.molstruc.2017.08.085
27. M. M. Lawal, T. Govender, G. E. Maguire, B. Honarparvar, and H. G. Kruger, *Journal of Molecular Modeling,* **22,** 235 (2016), https://doi.org/10.1007/s00894-016-3084-z
28. L. Gummidi, N. Kerru, C. U. Ibeji, and P. Singh, *Journal of Molecular Structure,* **1187,** 50(2019), https://doi.org/10.1016/j.molstruc.2019.03.053
29. J. J. McKinnon, M. A. Spackman, and A. S. Mitchell, *Acta Crystallographica,* **B60,** 627(2004), https://doi.org/10.1107/S0108768104020300
30. C. F. Mackenzie, P. R. Spackman, D. Jayatilaka and M. A. Spackman, *IUCrJ,* **4,** 575(2017), https://doi.org/10.1107/S205225251700848X
31. A. D. Becke, *The Journal of Chemical Physics,* 98, 1372(1993), https://doi.org/10.1063/1.464304
32. C. Lee, W. Yang and R. G. Parr, *Physical Review B,* **37,** 785 (1998), https://doi.org/10.1103/PhysRevB.37.785
33. A. Abbas, H. Gökce and S. Bahçeli. *Spectrochimica Acta, Part A,* **152**, 596(2016), https://doi.org/10.1016/j.saa.2015.01.099
34. G. Yuan, K. Z. Shao, D. Y. Du, X. L. Wang, Z. M. Su and J. F. Ma. *CrystEngComm,* **14**, 1865(2012), https://doi.org/10.1039/c1ce06178j

[RJC- 8667/2024]